Journal of
Environmental Science
and Technology

A Review of Laboratory and Numerical Simulations of Hydrocarbons Migration in Subsurface Environments

[1]S.A. Kamaruddin, [2]W.N.A. Sulaiman, [3]N.A. Rahman, [2]M.P. Zakaria, [4]M. Mustaffar and [3]R. Sa'ari

[1]Department of Civil Engineering, UTM Razak School of Engineering and Advanced Technology, Universiti Teknologi Malaysia International Campus, Kuala Lumpur, Malaysia
[2]Department of Environmental Sciences, Faculty of Environmental Studies, Universiti Putra Malaysia, UPM Serdang, Selangor, Malaysia
[3]Department of Hydraulics and Hydrology, Faculty of Civil Engineering, Universiti Teknologi Malaysia, UTM Skudai, Johor, Malaysia
[4]Survey Unit, Faculty of Civil Engineering, Universiti Teknologi Malaysia, UTM Skudai, Johor, Malaysia

Corresponding Author: Samira Albati Kamaruddin, Department of Civil Engineering, UTM Razak School of Engineering and Advanced Technology, Universiti Teknologi Malaysia International Campus, Jalan Semarak, 54100 Kuala Lumpur, Malaysia Tel: (603) 26154617 Fax: (603) 26934844

ABSTRACT

The leaking from underground storage and surface spills of various hydrocarbon sources has caused the hazardous subsurface contamination. The toxic compounds of chemicals have made field study infeasible and it has been replaced by laboratory and numerical simulations. This study introduces the methodology for two-dimensional non-aqueous phase liquid experiments with the application of light reflection and light transmission methods associated with image analysis methods. In addition, this study emphasizes the experiments with numerical simulations in which data acquisition is essential for verification and validation of numerical models. The numerical efforts are supported by basic formulation, with existing codes and its application for light hydrocarbon migration simulation. Overall, this study discussed the laboratory works and numerical simulations using current visualization techniques and makes suggestions for future research.

Key words: Non-aqueous phase liquid, multiphase flow, laboratory, numerical simulation, porous media

INTRODUCTION

Leaking and spills of hydrocarbons through the Earth's subsurface have caused serious problems, resulting in groundwater contamination and making groundwater toxic and unsafe for drinking water and irrigation purposes. Most hydrocarbons in subsurface soil are characterized as immiscible and form a liquid phase separate from water and/or air. Non-aqueous phase liquids (NAPLs) and polycyclic aromatic hydrocarbons (PAHs) are the two groups of hydrocarbon contaminants that are being studied by the researchers in Malaysia. The previous research shows that petrogenic sources of PAHs have been severely polluted Malaysian aquatic environments (Zakaria *et al.*, 2002; Sakari *et al.*, 2008). When the same sources spilled on the ground it creates NAPLs contaminant and some multicomponent NAPLs contain PAHs.

Commonly, two types of NAPLs can contaminate the subsurface environments. The lighter hydrocarbons, with a density less than that of water, are classified as light non-aqueous phase liquids (LNAPLs) and the heavier ones that are denser than water are classified as dense non-aqueous phase liquids (DNAPLs). The LNAPL pass through unsaturated soil and float on the surface of groundwater while DNAPL move downward through the saturated soil to settle. Geologic configuration is the key to disposition of NAPLs in the subsurface. For LNAPL, its movement in the unsaturated zone is of primary importance because the bulk liquid does not penetrate the saturated zone. In contrast, the structure of both saturated and unsaturated regions has a major impact on DNAPL disposition. Thus, LNAPL laboratory experiments under controlled conditions associated with numerical simulations focus mainly on the unsaturated region.

During the past two decades, much more information has become available on laboratory and numerical simulations of NAPL. Mercer and Cohen (1990) published the review on properties, characterization and remediation of NAPL. They claimed that future research would require better in-situ measurement of NAPL properties along with an improved understanding of mass-transfer mechanisms in NAPL modeling. Following these recommendations should provide better NAPL characterization and increasing remediation technologies, as well as field-scale guidance for site investigations. Concerned by insufficient field-scale data collection, Gelhar *et al.* (1992) published a critical review of dispersivity observations from 59 different field sites, compiling variations of aquifer characteristics and dispersivity determination. Summarizing experimental work, Chevalier and Petersen (1999) provided an overview of NAPL flow, transport and remedial techniques in two-dimensional (2-D) laboratory aquifer models. However, this review only discusses literature published up to 1997.

Karapanagioti *et al.* (2003) have reviewed the codes and usage in NAPL studies covering modeling of volatile organic compounds (VOCs). Six codes were selected for extensive review from nineteen public domain models, including 1-D (McCarthy, 1992; McCarthy and Johnson, 1993), MOFAT (Katyal *et al.*, 1991), NAPL simulator (Guarnaccia *et al.*, 1997), R-UNSAT (Lahvis and Baehr, 1997), VENT2D (Benson, 1994; Benson *et al.*, 1993) and VLEACH (Ravi and Johnson, 1997). As a result, Karapanagioti *et al.* (2003) found several code shortcomings and suggested further modeling revisions while keeping the computational requirements reasonable. Considering the available VOC models, NAPL studies most likely have moved beyond the non-volatile three-phase code (i.e., STOMP) published by White and Oostrom (1997, 2000).

Considering hydrocarbons as the main source of LNAPL, Saleem *et al.* (2004) presented the state-of-the-art techniques for determination of spilled hydrocarbon volume using both direct methods and indirect methods. These authors suggested the necessity of interdisciplinary cooperation between investigators from engineering as well as the sciences. The most recent collective reviews on multidimensional, multifluid, intermediate-scale experiments cover experimental aspects of NAPL dissolution and enhanced remediation (Oostrom *et al.*, 2006a), in addition to flow behavior, saturation imaging and tracer detection and quantification (Oostrom *et al.*, 2007). These reviews have provided comprehensive discussion on 2-D laboratory-scale research without emphasizing the numerical simulation exercises and visualization of results.

This study aims to introduce the existing 2-D laboratory and numerical simulations of LNAPL including the process of visualizing simulation results that has improved on lengthy and tedious conventional methods. Thus, the findings will benefit future laboratory and numerical simulations as well as highlighting the present technology in this field. Through this effort, future researchers may find a better way of providing prediction models for subsurface environments.

EXPERIMENTAL

NAPL experimental: Previously, researchers have used various terms for physical aquifer models. For the purpose of this review, we use the term flow cells to refer to the aquifer models, while the term sand tank refers to the built tank with packed sand. In performing NAPL experiments, they should be categorized according to purpose: laboratory investigation or numerical validation. For laboratory setup, numerous methods are available in the literature; however, the selection of an experimental setup normally depends on the applicability and required level of accuracy. Finally, without measurement of liquid pressures and saturations, especially by using the saturation imaging technique, data acquisition would be impossible.

Oostrom *et al.* (2007) have discussed the categories of flow behavior experiments as shown in Fig. 1. Each category of qualitative and quantitative infiltration and redistribution experiments,
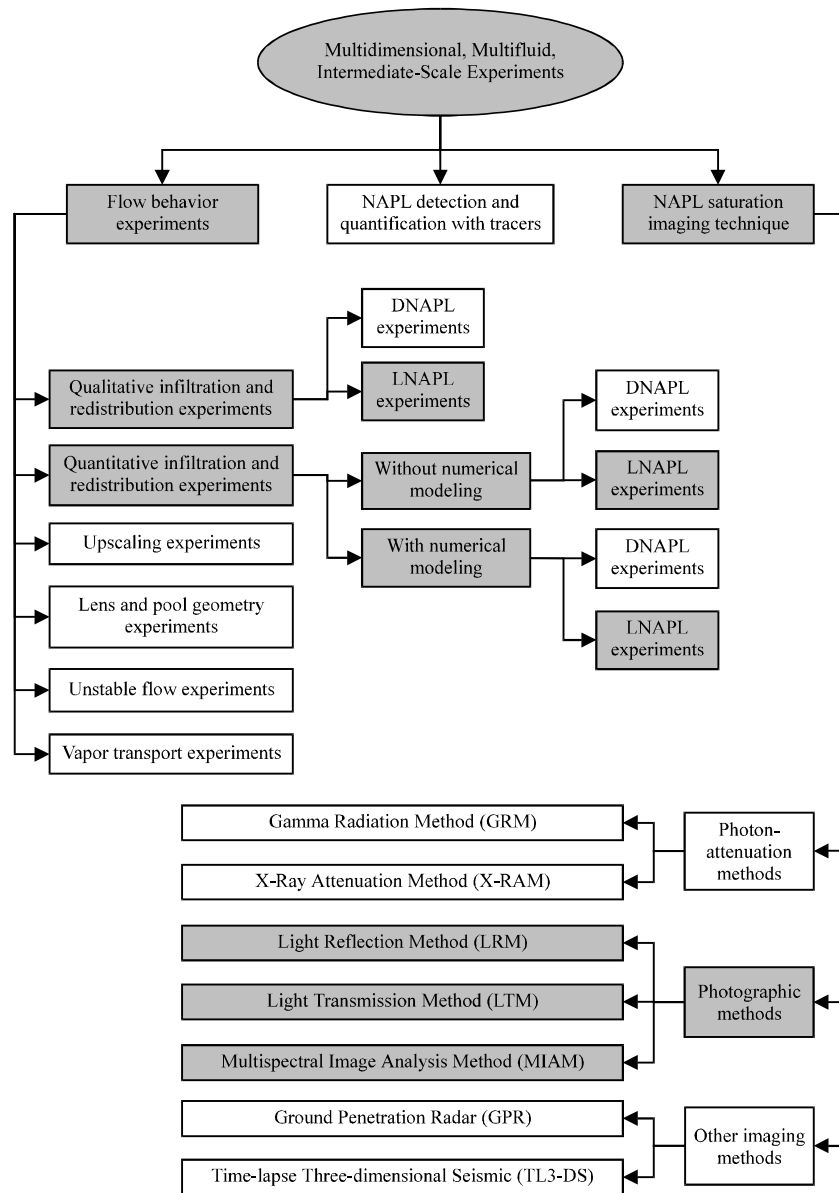

Fig. 1: Highlighted methods of NAPL experiments from Oostrom *et al.* (2007)

with and without numerical modeling, is divided into DNAPL and LNAPL experiments. The experimental information with grey background (Fig. 1) shows the selected interests in qualitative and quantitative LNAPL experiments and photographic methods for NAPL saturation imaging technique. Since this review concerns only LNAPL flow behavior experiments, twenty research papers (Table 1) have been selected to highlight the analysis carried out in the experimental and numerical simulations. In the qualitative LNAPL experiments, the flow behavior of NAPL was observed without data acquisition for saturation mapping and no data were presented for numerical simulation. The final group in the list of LNAPL infiltration and redistribution experiments denotes those studies that applied numerical models such as a simple numerical

Table 1: Qualitative and quantitative infiltration and redistribution of LNAPL experiments in the unsaturated zone with and without numerical modeling

Size of sand tank (H×L×W)[a] in cm	Wall material	Porous media	LNAPL	Amount of LNAPL	Saturation imaging[d]	Reference
Qualitative infiltration and redistribution of LNAPL experiments						
80×260×20 105×105×15	Glass	Heterogeneous	Heating oil, kerosene	-	-	Schwille (1967)
120×69×1.27	Glass	Homogeneous; heterogeneous	Soltrol 110	1.248 L	-	Catalan and Dullien (1995)
60×50×0.95	Glass	Homogeneous	Soltrol 220	0.01-0.02 L	LTM	Schroth *et al.* (1998a)
68×112×3	Glass[b]; stainless steel[c]	Homogeneous	Gasoline	0.035 L min^{-1}	-	McDowell and Powers (2003)
Quantitative infiltration and redistribution of LNAPL experiments without numerical modeling						
61×71×5	Glass, Lucite[b]; stainless steel[c]	Homogeneous; heterogeneous	Kerosene	0.35 L	-	Pantazidou and Sitar (1993)
120×150×6	Glass[b]; aluminum[c]	Homogeneous	*n*-heptane	2.0 L	LRM	Van Geel and Sykes (1994b)
122-183×975 ×5.08	Plexiglas[b]; stainless steel[c]	Homogeneous; heterogeneous	Soltrol 220	Varies	GRM	Illangasekare *et al.* (1995)
100×100×5	Glass	Homogeneous	Gasoline	0.03 L min^{-1}	-	Chevalier (1998)
180×120×8	Glass[b]; Perspex[c]	Homogeneous; heterogeneous	Soltrol 220	3.0 L	MIAM	Kechavarzi *et al.* (2000)
180×120×8	Glass[b]; Perspex[c]	Homogeneous	Soltrol 220	3.0 L	MIAM	Kechavarzi *et al.* (2005)
180×120×8 `	Glass[b]; Perspex[c]	Heterogeneous	Soltrol 220	4.0 L	MIAM	Kechavarzi *et al.* (2008)
Quantitative infiltration and redistribution of LNAPL experiments with numerical modeling						
40×90×5	Plexiglas	Homogeneous	Soltrol C, transmission oil	-	-	Hochmuth and Sunada (1985)
100×100×8	Plexiglas	Homogeneous	Bayoil 82	4.0 L	GRM	Host-Madsen and Jensen (1992)
24×24×24	Acrylic	Homogeneous	Soltrol 220, mineral oil	0.5 L	-	Simmons *et al.* (1992)
100×167×5	Glass[b]; kynar[c]	Homogeneous	Soltrol 220	0.825 L	GRM	Oostrom *et al.* (1997)
120×150×6	Glass[b]; aluminum[c]	Homogeneous	*n*-heptane	2.0 L	LRM	Van Geel and Sykes (1997)
108×152×8.2	Ultem plastic	Homogeneous	Soltrol 130	15 L	GRM	Waddill and Parker (1997)
60×50×1	Glass	Heterogeneous	Soltrol 220	0.01-0.02 L	LTM	Schroth *et al.* (1998b)
40×40×2.5	Plexiglas	Heterogeneous	Jet fuel A-1	0.015 L	-	Wipfler *et al.* (2004)
75×102×5.5	Glass	Homogeneous	Lard oil	0.4 L	GRM	Oostrom *et al.* (2006b)

[a]H×L×W: height×length×width. [b]Front wall. [c]Back wall. [d]LTM: light transmission method with no saturation mapping; LRM: light reflection method; GRM: gamma radiation method; MIAM: multispectral image analysis method

model (Hochmuth and Sunada, 1985), ECLIPSE (Høst-Madsen and Jensen, 1992), IMPES (Van Geel and Sykes, 1997), ARMOS (Waddill and Parker, 1997) and STOMP (Oostrom *et al.*, 1997; Oostrom *et al.*, 2006b; Simmons *et al.*, 1992; Wipfler *et al.*, 2004).

For a quantitative experiment, data acquisition is essential for numerical simulations in order to verify and validate numerical models. Thus, we emphasize here the experiments with numerical simulations.

Laboratory setup: For the purpose of laboratory setup in quantitative experiments, materials and methods need to be specifically determined for flow cells, porous media, LNAPL source and fluid measurement devices. The size of sand tanks used for intermediate-scale LNAPL (Table 1) begins with the tank height instead of the length, in order to obtain the actual size of the fabricated sand tank. For instance, Kechavarzi *et al.* (2005, 2008, 2000) used the same 180 cm-high x 120 cm-long x 8 cm-wide sand tank dimension, but the actual height of flow cells were varied among the three reported experiments. The types and thicknesses of wall materials are also important in the quest to provide better visualization for image acquisition and sensor ports installation. Sand tank walls have been made from glass, Plexiglas, Perspex, acrylic, Ultem plastic, kynar, aluminum and stainless steel.

The properties of porous media play an important role in numerical simulations. Determination of porosity, saturated conductivity and other soil properties is vital to determining input parameters for numerical models. The sand used for intermediate-scale LNAPL is normally washed and dried; it can be oven-dried at 45°C for 48 h (Niemet and Selker, 2001). Moisture content measurements after oven drying verified that the moisture content of the sands was negligible (Bob *et al.*, 2008).

Sand-packing techniques are important to achieve uniform soil condition with respect to bulk density. Previously, a removable plastic sleeve method can be used for homogeneous packing and the standard drop sieve method can be used for heterogeneous packing (Illangasekare *et al.*, 1995). In the removable sleeve method, a plastic liner is inserted into the column and the sand is poured gradually from the liner. The liner is then pulled evenly from the flume to produce a uniform settling. For dry sand-packing, used a prismatic funnel called a hopper was used to fill the tank at a continuous and uniform rate (Niemet and Selker, 2001). The hopper was the same width as the tank and contained two coarse screens to randomize the trajectories of the falling sand particles. The overburden fill was removed by vacuum.

The typical properties of porous media are the mean size (D_{50}), coefficient of uniformity (C_U), porosity (ϕ), conductivity (K_s) and Van Genuchten parameters (α, n). The related properties are collected as tabulated in Table 2, some values in the table can be compared to the typical values of capillary pressure curve parameters and vertical hydraulic conductivities for a variety of soil types provided by Katyal *et al.* (1991).

The source of LNAPL such as gasoline has multiple constituents of non-inert oil as given in aromatics volatile organics: for instance, benzene, toluene, ethyl-benzene and xylene (BTEX) (Table 3). Table 3 shows the physical and chemical properties of selected organic compounds (Chevron Philips Chemical Company LP., 2009; Katyal *et al.*, 1991; Kechavarzi *et al.*, 2005; Mercer and Cohen, 1990; USEPA, 1991) that are significantly contaminating the subsurface environment and Soltrol 220 (Chevron Philips Chemical Company LP., 2009; Kechavarzi *et al.*, 2005), all of which are widely used in LNAPL experiments. Table 4 gives the properties of LNAPL that originate from petroleum products (Mercer and Cohen, 1990).

Table 2: Porous media properties for infiltration and redistribution of LNAPL experiments

Porous media (Supplier)	Grade of sand	Range and D_{50} (mm)	$C_U = \dfrac{D_{60}}{D_{10}}$	Porosity	Conductivity/ permeability	Van Genuchten parameter α (cm^{-1})	n	Reference
Barco sand (Barnes Co., Waterdown, Ontario, Canada)	Barco 71	0.076-0.42 (0.220)	-	0.381	15 µm^2	-	-	Catalan and Dullien (1995)
Accusand silica sand (Unimin Corp. Le Sueur, MN, US)	12/20	1.105	1.231	-	24.7 cm min^{-1}	0.151	7.35	Schroth *et al.* (1996)
	20/30	0.713	1.19	-	29.5 cm min^{-1}	0.0995	10.57	
	30/40	0.532	1.207	-	31.4 cm min^{-1}	0.0679	13.10	
	40/50	0.359	1.20	-	33.4 cm min^{-1}	0.0453	12.18	
Quartz sand (U.S. Silica, Ottawa, IL)	Mix. 1	0.035	2.466	0.376	0.037 cm sec^{-1}	-	-	McDowell and Powers (2003)
	Mix. 2	0.033	1.333	0.391	0.079 cm sec^{-1}	-	-	
Crystal silica sand (southern California)	Coarse 30	0.25	-	0.43	0.159 cm sec^{-1}	-	-	Pantazidou and Sitar (1993)
	Fine 60	0.45	-	0.44	0.039 cm sec^{-1}	-	-	
Well-sorted silica sand	-	-	-	0.374	1·10^{-4} m sec^{-1} (K$_z$) 2·10^{-4} m sec^{-1} (K$_x$)	0.0203	6.49	Van Geel and Sykes (1994b)
White silica sand (Unimen Sillica)	No. 8	1.50	1.39	-	0.01200 m sec^{-1}	-	-	Illangasekare *et al.* (1995)
	No. 16	0.88	1.72	-	0.00430 m sec^{-1}	-	-	
	No. 30	0.49	1.50	-	0.00145 m sec^{-1}	-	-	
	No. 70	0.19	1.86	-	0.00024 m sec^{-1}	-	-	
Ottawa sand (Soiltest, Lake Bluff, III)	Mesh 40	-	-	0.38	0.102 cm sec^{-1}	-	-	Chevalier (1998)
Uniform silica sand (Hepworth Minerals and Chemicals, UK)	Frac. D BS4500	0.09-0.15 (0.14)	1.35	0.42	12.6 m day^{-1}	0.01494	14.43	Kechavarzi *et al.* (2000)
	Frac. E BS4500	0.15-0.30 (0.225)	1.74	0.41	40.7 m day^{-1}	0.02026	12.27	
Well-graded natural quarry sand	RH65	0.10-0.60 (0.245)	2.07	0.38	12.5 m day^{-1}	0.02127	9.15	
Uniform sand	Sand 1	0.178	-	0.39	1.14·10^{-11} m^2	-	21.7	Host-Madsen and Jensen (1992)
	Sand 3	0.558	-	0.39	8.17·10^{-11} m^2	-	14.2	
Well-graded white quartz sand (AWK, Germany)	Fine	0.7-1.2	-	0.55	0.05 cm sec^{-1}	0.08	3.9	Wipfler *et al.* (2004)
	Coarse	1.0-1.8	-	0.52	0.09 cm sec^{-1}	0.27	5.9	
Accusand silica sand	40/50	-	-	0.34	3.24·10^{-11} m^2	-	-	Oostrom *et al.* (2006b)

The selection of LNAPL source is dependent on the numerical models to be used in the simulations as well as the types of constituents present in the LNAPL contamination. For example, the STOMP code is applied for non-volatile LNAPL sources such as Soltrol® and jet fuel; this code is also known as Non-Volatile Three-Phase (NVTP) operational code and is not applicable to multi-component organic compound mixtures. In the past, LNAPL has been dyed with Sudan® III at 0.01% by weight (Schroth *et al.*, 1998a, b) to enhance the LNAPL delineation in porous media.

Saturation imaging techniques: In the laboratory, measurement of NAPL saturation is the most difficult and important task in acquiring precise data. For most researchers, a critical review of NAPL saturation imaging techniques is of primary concern. Oostrom *et al.* (2007) discussed seven

Table 3: Physical and chemical properties of selected LNAPL from aromatic nonhalogenated volatile organics and solvent at 20°C (unless noted)

Organic compound	Nonhalogenated volatile organic (aromatics)							Solvent
	Benzene	Ethyl-benzene	Styrene	Toluene	m-xylene	o-xylene	p-xylene	Soltrol 220[e]
Specific gravity	0.878[a] 0.8737[b (2)]	0.867[a]	0.906[b]	0.867[a] 0.8623[b (2)]	0.8642[b]	0.880[a]	0.8611[b]	0.7899[e (1)]
Dynamic viscosity (cp)	0.6468[c] 0.6028[b(2)]	0.678[c]	0.751[c]	0.58[c]	0.608[c]	0.802[c]	0.635[c]	4.8[d]
Surface tension (dyne cm^{-1})	27.90[a]	29.20[a]	32.30[b]	29.00[a]	-	31.21[a]	-	-
Interfacial tension (dyne cm^{-1})	28.88[a]	35.48[a]	35.50[b]	36.10[a]	36.40[b]	36.06[a]	37.80[b]	36.00[d]
Vapor pressure (mmHg)	95.2[b]	7[b]	4.5[b]	28.1[b]	10[b]	6.6[b]	10[b]	0.36[e(3)]
Log K$_{ow}$	2.13[c]	3.15[c]	3.16[c]	2.73[c]	3.20[c]	3.12[c]	3.15[c]	-
Log K$_{oc}$	1.81[c]	2.83[c]	-	2.41[c]	2.84[c]	2.84[c]	2.84[c]	-
Water solubility (mg L^{-1})	1780[a]	152[a]	300[c]	515[a]	200[c]	170[c]	198[c]	0
Henry's constant (atm·m^3 mol^{-1})	5.59·10^{-3b}	6.43·10^{-3b}	2.05·10^{-3b}	6.37·10^{-3b}	1.07·10^{-2b}	5.10·10^{-3b}	7.05·10^{-3b}	-
Diffusion coefficient in water (m^2 day^{-1})	9.42·10^{-5a}	6.21·10^{-5a}	-	8.21·10^{-5a}	-	6.21·10^{-5a}	-	-
Diffusion coefficient in air (m^2 day^{-1})	0.763[a]	0.61[a]	-	0.68[a]	-	0.61[a]	-	-
Diffusion coefficient in oil (m^2 day^{-1})	1.13·10^{-4a}	-	-	9.87·10^{-5a}	-	7.00·10^{-5a}	-	-
Oil-water partition coefficient	493[a]	-	-	1683[a]	-	5729[a]	-	-
Air-water partition coefficient	0.24[a]	-	-	0.28[a]	-	0.22[a]	-	-
Density (g m^{-3})	0.8765·10^{6c}	0.8670·10^{6c}	0.9060·10^{6c}	0.8669·10^{6c}	0.8642·10^{6c}	0.8800·10^{6c}	0.8610·10^{6c}	0.7900·10^{c}

[a]Katyal *et al.* (1991); [b]Mercer and Cohen (1990), [c]USEPA (1991), [d]Kechavarzi *et al.* (2005), [e]Chevron Philips Chemical Company LP (2009); [(1)]value is at 15.6°C; [(2)]value is at 25°C; [(3)]value is at 37.8°C

Table 4: Physical and chemical properties of selected LNAPL from hydrocarbon/petroleum products at 20°C (Mercer and Cohen, 1990)

Product	Automotive gasoline	#1 fuel oil	#2 fuel oil	Mineral oil	n-heptane	n-hexane	n-nonane	n-octane	n-pentane
Specific gravity	0.7321	0.81-0.85	0.88	0.822	0.6838	0.6603	0.7176	0.7025	0.626
Dynamic viscosity (cp)	0.45	2.05	5.92	-	0.409	0.33	0.7160	0.542	0.225
Surface tension (dyne cm^{-1})	21	27	25	25	19.3	18.4	22.9	21.7	16
Interfacial tension (dyne cm^{-1})	50	48	50	50	50.2	51	35	50.8	50.2

imaging techniques (Fig. 1). They found that most experiments used photon-attenuation methods such as gamma and X-ray techniques due to the accuracy and precision of these methods. Photographic methods such as the Light Reflection Method (LRM), the Light Transmission Method (LTM) and the Multispectral Image Analysis Method (MIAM) provide alternatives for researchers to select non-destructive and non-intrusive tool techniques. Another two methods that may be useful but that need further development for laboratory applications are Ground-Penetrating Radar (GPR) and three-dimensional seismic imaging. Methodological reviews were followed by NAPL detection and quantification with tracers. Previously, researchers had used partitioning tracer methods for detecting and quantifying NAPL saturation at large-scale. Workers in the petroleum industry were the first to use partitioning and non-partitioning tracers simultaneously through injection in aquifers. Oostrom *et al.* (2007) concluded that this application needed more experimental review, addressed by a team experienced with both laboratory and field conditions.

Considering experimental demands (Kechavarzi *et al.*, 2005) and other limitations, such as slow measurements and the hazards of working with high energy sources related to the photon-attenuation technique (Bob *et al.*, 2008), in conjunction with the latest Information Technology (IT) and software, more researchers have been searching for non-destructive and non-intrusive

techniques. Quantification of NAPL saturation has been carried out by using LTM (Conrad *et al.*, 2002; Darnault *et al.*, 1998, 2001; Flores *et al.*, 2007; Glass *et al.*, 2000) the LRM (O'Carroll *et al.*, 2004; Van Geel and Sykes, 1994a) and the MIAM (Kechavarzi *et al.*, 2000, 2005, 2008). All photographic methods acquire images by using either a digital camera or video camera depending on the required image specification for later processing.

NUMERICAL SIMULATIONS

The numerical simulations should begin with an understanding of the theoretical formulation behind the most common codes and numerical models. Based on this formulation, Lewis *et al.* (1998) and Rahman and Lewis (1999) developed a numerical model that describes the flow of multiphase immiscible fluids in a deforming porous medium (Lewis and Schrefler, 1998). In the validation exercises, a numerical example of 2-D multiphase flow also demonstrates the impact of NAPL leaking in a porous medium that has also been subjected to water infiltration. In addition, a numerical modeling was carried out and tested to local soil samples to further understand the multiphase flow and pollutant transport in deformable porous materials (Rahman *et al.*, 2001, 2002). Historically, the basic formulation of NAPL was developed without considering the effect of hysteresis. As natural phenomena are normally affected by the fluid entrapment and saturation hysteresis, ignoring this effect may contribute to greater error in simulating the natural LNAPL subsurface contamination.

Theoretical formulation: The theoretical understanding for LNAPL in porous media was developed by taking into consideration multiphase flow formulation, mass continuity and constitutive relationships. The constitutive relationships are comprised of capillary pressure and saturation (dimensionless capillary pressure, three-phase capillary pressure and saturation), relative permeability and saturation (three-phase relative permeability), treatment of trapped fluid phases and hysteresis (capillary pressure-saturation and relative permeability-saturation).

Multiphase flow: In multiphase flow where immiscible fluids exist in a porous medium, the interfacial tension occurs from the interactions among fluid phases. This tension is a result of imbalanced attractive forces between the molecules at the interface. In the subsurface, adhesive forces occur between fluids and solids. The most preferred fluid that successfully coats the grain surfaces is called the wetting fluid, while the weakest adhesive attraction fluid is called the non-wetting fluid (Fetter, 1999). The greater affinity of the wetting phase for the solid medium produces suction on this phase into smaller pore spaces that create the phenomenon of capillarity. The theory of capillarity was first discussed by Leverett (1941). Based on Corey (1994), the capillary pressure, P_C is given by:

$$P_C = P_n - P_w = \frac{2\sigma\cos\theta}{r} \qquad (1)$$

where, P_n is the pressure in non-wetting phase, P_w is the pressure in wetting phase, σ is the interfacial tension, θ is the contact angle and r is the effective pore radius.

Multiphase flow formulation from Bear (1972) stated the general flow equation for any phase, α, as:

$$q_{\alpha i} = -k_{r\alpha} \frac{k_{ij}}{\mu_{\alpha}} \left[\frac{\partial P_{\alpha}}{\partial x_j} + \rho_{\alpha} g \frac{\partial z}{\partial x_j} \right] \qquad i,j = 1,2,3 \tag{2}$$

where α is the fluid phase of either water, gas, or NAPL (W, G, or N); q is the Darcy flux in the i coordinate direction; k_r is the relative permeability; k_{ij} is the intrinsic permeability tensor; P is the fluid pressure; z is the vertical direction; x_j is the coordinate direction; μ is dynamic viscosity; ρ is the fluid density; and g is the gravitational acceleration.

For mass continuity, Parker (1989) stated the law of mass conservation for each fluid phase as:

$$\varphi \frac{\partial \rho_{\alpha} S_{\alpha}}{\partial t} = -\frac{\partial \rho_{\alpha} q_{\alpha i}}{\partial x_i} + Q_{\alpha} \quad i = 1,2,3 \tag{3}$$

where, ϕ is the effective porosity, ρ is the fluid phase density, S_{α} is the phase saturation, t is time and Q_{α} is the source or sink term for a mass flux.

By substitution of Darcy's Law (Eq. 2) in Eq. 3, therefore:

$$\varphi \frac{\partial \rho_{\alpha} S_{\alpha}}{\partial t} = \frac{\partial}{\partial x_i} \left[\rho_{\alpha} \frac{k_{r\alpha} k_{ij}}{\mu_{\alpha}} \left(\frac{\partial P_{\alpha}}{\partial x_j} + \rho_{\alpha} g \frac{\partial z}{\partial x_j} \right) \right] + Q_{\alpha} \quad i,j = 1,2,3 \tag{4}$$

where, the sum of saturations is assumed equal to one:

$$S_W + S_N + S_G = 1 \tag{5}$$

and capillary pressure is defined as:

$$P_{C_{GW}} = P_G - P_W$$
$$P_{C_{NW}} = P_N - P_W$$
$$P_{C_{GN}} = P_G - P_N \tag{6}$$

In the multiphase fluid flow, the order of fluid wettability from the highest to the lowest is water, followed by NAPL and gas.

Constitutive relationships: The constitutive relationships are developed from the link of fluid saturation to capillary pressure-saturation (P-S) and relative permeability-saturation (k-S). The relationship of P-S can be determined by using various methods and the most two common methods used in hydrogeology (BC and VG) are derived from the work of Broorks and Corey (1964) and Van Genuchten (1980). The critical distinction between VG and BC models is that the VG model calculates a non-wetting phase saturation greater than 0 as soon as NAPL pressure exceeds water pressure, while the BC model has a distinct displacement pressure, p_d. Both methods use the concept of effective saturation that is used to scale the phase saturation values by the endpoints or the maximum saturation range possible, which is dependent on the residual saturation (Broorks and Corey, 1964; Van Genuchten, 1980):

$$\overline{S}_\alpha = \frac{S_\alpha - S_m}{1 - S_m} \qquad (7)$$

where, $\overline{S}_\alpha$ is the effective fluid saturation for the phase; S_α is the total saturation of phase and S_m is the residual water saturation.

Capillary pressure-saturation relationship: This relationship can be developed by referring to Van Genuchten (1980) and quoting Mualem (1976):

$$\overline{S}_\alpha = \left[\frac{1}{1 + (\alpha P_C)^n} \right]^m \qquad (8)$$

where, α and n are the fitting parameters and $m = \left(1 - \frac{1}{n} \right)$. Whereas, according to Broorks and Corey (1964):

$$\overline{S}_\alpha = \left(\frac{P_C}{P_d} \right)^{-\lambda} \qquad (9)$$

where, λ is a fitting parameter for the pore size distribution index and P_d is the displacement pressure.

The three-phase P-S is rarely determined through experimental means because it is extremely difficult to measure phase saturations and pressures in a three-phase system that possibly has many more fluid displacement combinations. The most common method used to produce three-phase P-S relationships is by an extension of two-phase systems as proposed by Leverett (1941).

A parametric model for three-phase k-S-P for monotonic drainage based on the work of Leverett (1941) and the Van Genuchten (1980) functional relationship was presented by Parker *et al.* (1987) that assumed water saturation in a three-phase system is dependent on the water-NAPL capillary pressure curve only:

$$\overline{S}_W = \left[\frac{1}{1 + \left(\alpha_{NW} P_{C_{NW}} \right)^n} \right]^m \quad \text{for} \ \ P_{C_{NW}} > 0 \qquad (10)$$

$$\overline{S}_W = 0 \ \ \text{for} \ \ P_{C_{NW}} \leq 0 \qquad (11)$$

where, the effective water saturation, $\overline{S}_w$ is defined as:

$$\overline{S}_W = \frac{S_W - S_{Wr}}{1 - S_{Wr}} \qquad (12)$$

where, $\overline{S}_{Wr}$ is the residual water saturation.

The second capillary pressure curve of interest is that of the gas-NAPL system. In a three-phase setting, the total wetting saturation (the sum of NAPL and water saturations) is a function of the gas-NAPL curve

$$\overline{S}_T = \left[\frac{1}{1+\left(\alpha_{GN} \, P_{C_{GN}}\right)^n} \right]^m \quad \text{for } P_{C_{GN}} > 0 \tag{13}$$

$$\overline{S}_T = 0 \quad \text{for } P_{C_{GN}} \leq 0 \tag{14}$$

where, $\overline{S}_T$ refers to the total wetting saturation, as the sum of the water and LNAPL saturations and the effective total wetting saturation, $\overline{S}_T$ is defined as:

$$\overline{S}_T = \frac{S_T - S_{Wr}}{1 - S_{Wr}} \tag{15}$$

The implicit assumption in Eq. 15 is that water is most wetting, followed by NAPL and then by gas. As a result, no interfaces between the water and gas phases exist until the NAPL phase reaches residual saturation. In the portions of the domain where NAPL is not present, the gas-NAPL curve equation, Eq. 14 is replaced with the two-phase term for water-gas capillary pressure, Eq. 8. A single P-S curve is often used in numerical models and scaled for the various phases through the interfacial tensions.

Relative permeability-saturation relationship: The relationship of k-S can be measured experimentally, with difficulty. Numerous relationships have been proposed for the continuous function in porous media and Broorks and Corey (1964) and Van Genuchten (1980) provide the most common expressions. For wetting phase and non-wetting phase relative permeability, Van Genuchten (1980) stated:

$$k_{rw} = \overline{S}_w^{\,1/2} \left[1 - \left(1 - \overline{S}_w^{\,1/m} \right)^m \right]^2 \tag{16}$$

$$k_{rn} = \left(1 - \overline{S}_n \right)^{1/2} \left[1 - \left(1 - \overline{S}_n^{\,1/m} \right) \right]^{2m} \tag{17}$$

while Broorks and Corey (1964) expressed these as:

$$k_{rw} = \overline{S}_w^{\,(2+3\lambda)/\lambda} \tag{18}$$

$$k_{rn} = \left(1 - \overline{S}_n \right)^2 \cdot \left(1 - \overline{S}_n^{\,(2+\lambda)/\lambda} \right) \tag{19}$$

In comparisons of both the k-S expressions, the BC model has provided a better experimental representation for LNAPL phase. This is because the BC model always calculates a lower k of

LNAPL than does the VG model, which over-estimates NAPL penetration speed and distance in the variably saturated porous medium. Both models used different pore-size distribution models in the k_r function derivations.

Laboratory measurement of the three-phase k-S relationship is also difficult, as is that of the P-S relationship. Based on Parker *et al.* (1987), water's relative permeability in a three-phase system is generally taken as a function solely of the water saturation. As the relationship of the wetting-phase, Eq. 16 is presumed to also be valid in air-water and NAPL-water systems, Mualem's model for the fluid phase of the intermediate wettability to air and water in a three-phase system (i.e., NAPL) is therefore:

$$k_{rN} = \left(\overline{S}_T - \overline{S}_W\right)^{1/2} \cdot \left\{\left(1 - \overline{S}_W^{1/m}\right)^m - \left(1 - \overline{S}_T^{1/m}\right)^m\right\}^2 \tag{20}$$

Hysteresis effect: Hysteresis in the context of multiphase flow refers to the dependence of the capillary pressure-saturation (P-S) relationship on the saturation history (Van Geel and Sykes, 1997). The wetting fluid is drained from the medium by an increase in p_c (drainage) or is entering the medium, expelling the non-wetting fluid (imbibition). The P-S hysteresis has four primary causes: (1) geometric or ink-bottle effects, (2) differences in contact angles during drainage and imbibition, (3) non-wetting-phase entrapment and (4) shrinking and swelling of the porous medium (Tindall and Kunkel, 1999).

Representation of the three-phase fluid relative k-S-P relationship is a critical component of multifluid flow simulation (Schroth *et al.*, 1998b). Parker *et al.* (1987) developed a constitutive k-S-P model for governing multiphase flow in porous media, based on Van Genuchten (1980) and Mualem (1976), known as the VGM model. White *et al.* (1995) used STOMP that incorporates the k-S-P model of Parker *et al.* (1987) along with two other k-S-P models. The first one is based on the two-fluid S-P model of BC and the pore-size distribution model of Burdine (1953) and is known as the BCB model. The second one is based on hysteretic VGM to form the HVGM model.

DISCUSSION

Image analysis for photographic methods: As mentioned earlier, the three photographic methods used for NAPL saturation measurement are gaining popularity among researchers (Table 5). Numerous measurements of fluid concentration and saturation have used photographic methods due to their advantages. The photographic technique can obtain images of a larger domain almost instantaneously without involving radiation energy. However, researchers may be subject to limited choices of porous media, as only silica sands and thinner flow cells will allow accurate image acquisitions (Oostrom *et al.*, 2007).

The use of the Light Reflection Method (LRM) and the Image Analysis Method (IAM) in image acquisition depend on each other. The LRM is the photographic technique used during the image acquisition or the setup of light reflection during the image collection (O'Carroll *et al.*, 2004; Schincariol *et al.*, 1993; Schincariol and Schwartz, 1990; Van Geel and Sykes, 1994a). Meanwhile, the IAM is the method used by researchers to process and analyze the captured images.

Previously, the LRM has been used to investigate NAPL infiltration under controlled lighting conditions such as using only two tungsten filament floodlights to illuminate the flume front wall in a dark room (Kechavarzi *et al.*, 2000; Van Geel and Sykes, 1994a). Problems such as reflections

Table 5: Measurement of fluid concentration and saturation using photographic method

Measurement	Size of tank (H×L×W)[a] in cm	Method[b]	Digital camera model[c]	Image analysis software	Reference
Concentration of Rhodamine WT	71×106.8×5	IAM	-	Tracor Northern 5500 Image Analysis Computer	Schincariol and Schwartz (1990)
Concentration distribution of dense NaCl	71×106.8×5	IAM	CCD camera	Digital Equipment Corporation Microvax II computer and Gould IP9527 image processor	Schincariol et al. (1993)
Saturation of n-heptane	120×150×6	LRM	-	EASI (P.C.I., Inc., Toronto, Ontario, Canada)	Van Geel and Sykes (1994b)
Fluid saturation distribution	180×120×8	MIAM	Kodak Professional DCS420IR	Image-Pro Plus software (Media Cybernetics, L.P.)	Kechavarzi et al. (2000)
Liquid saturation	60×50×1.27	LTM	CCD camera (ISI Systems, Santa Barbara, CA) with a Kodak KAF0400	Transform 3.4 (Fortner Software LLC)	Niemet and Selker (2001)
Colloids concentration plume	60×50×1.27	LTM	CCD camera (ISI Systems, Santa Barbara, CA) with a Kodak KAF0400	Transform 3.4 (Fortner Software LLC)	Weisbrod et al. (2003)
Concentration distribution of Rhodamine WT	1.25 m×6.25 m ×0.05 m	IAM	CCD camera	MATLAB	McNeil et al. (2006)
Colloids concentration plume	20×10×0.67	TLFI	CCD camera (Hitachi KP-D581, Hitachi-Denshi UK)	Data Translation, UK and Surfer 8.0 software (Golden Software, CA)	Bridge et al. (2006)
Saturation of undyed tetrachloroethylene (PCE)	15.24×15.25×1.40 48.26×48.26×1.40	LTM	CCD camera (Model Number 7486-0002, Princeton Instruments, Trenton, NJ)	Image-Pro Plus software (Media Cybernetics Inc., Silver Spring, MD)	Bob et al. (2008)
Concentration of salt-dye solutions	60×158×4	LTM	Nikon D70	Nikon camera control-PRO	Konz et al. (2008)

[a]H×L×W: height×length×width. [b]IAM: image analysis method; LRM: light reflection method; MIAM: multispectral image analysis method; LTM: light transmission method; TLFI: time-lapse fluorescent imaging. [c]CCD: charge-coupled device

of the camera or other peripheral equipment on the sand tank walls can be eliminated by placing a black curtain or sheet of black felt in front of the tank. Photographs are taken through a slit or hole in the curtain, as shown in Fig. 2.

In the IAM, McNeil *et al.* (2006) have extended the image processing steps (Fig. 3) of Schincariol *et al.* (1993) to accommodate heterogeneous media conditions. Because of the many calibration procedures involved, the processing tools used previously, such as Image-Pro Plus software (Media Cybernetics Inc.) and MATLAB®, can overcome this drawback in image processing steps. To our knowledge, McNeil *et al.* (2006) have used MATLAB® in the image analysis processing steps and the script package can be obtained by contacting the authors. This means that more studies can be extended to improve the image processing steps using the MATLAB environment.

The LTM (also called light transmission visualization, or LTV) was first developed by Hoa (1981) and improved by Tidwell and Glass (1994) in order to measure water saturation and was subsequently modified by Bob *et al.* (2008) for DNAPL saturation measurement. The LTM was usually conducted using a smaller flow cell, -complete with cooling fan and, -lighting source, where this was built in an experimental chamber frame (Niemet and Selker, 2001; Weisbrod *et al.*, 2003). A thermoelectrically air-cooled Charge-Coupled Device (CCD) camera was used to collect images using a determined-wavelength band-pass filter.
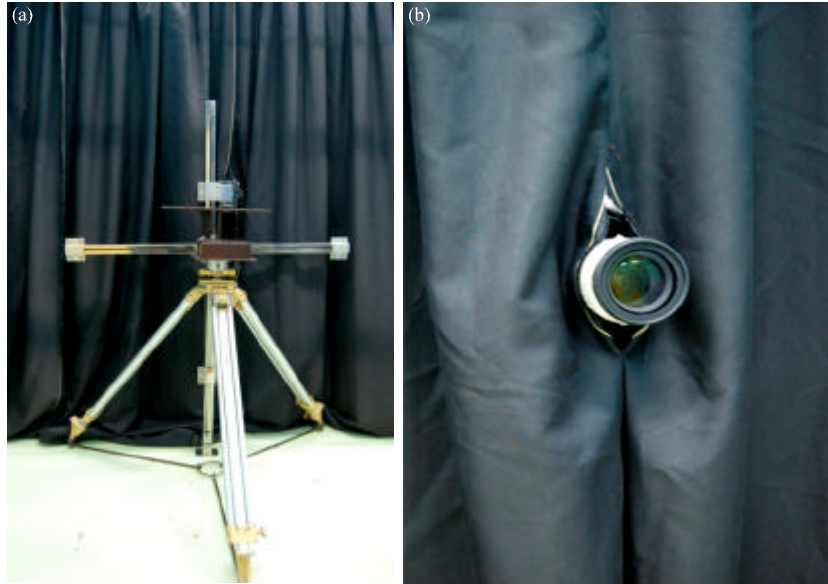
Fig. 2: Placement of a digital camera through a slit of black curtain. (a) A digital camera at one side of curtain and (b) camera lens at another side of curtain
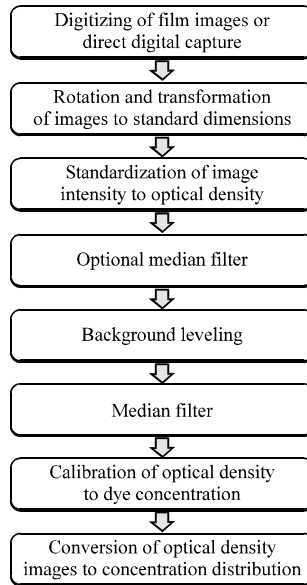

Fig. 3: Basic image processing steps given by McNeil *et al.* (2006) that has been modified from Schincariol *et al.* (1993)

Numerical models and its application: To date, many numerical models are available for NAPL simulations (Table 6). These models are capable of performing multidimensional analysis based on Finite Difference (FD) (i.e., UTCHEM, TOUGH2, STOMP) or the Finite Element (FE) method (i.e., MOFAT, NAPL Simulator). There are valid reasons for choosing either the FD or FE method for variably saturated flow solution. However, the choice is largely personal and proponents of a

Table 6: Existing two-dimensional numerical models designed primarily for NAPL simulations

Numerical model	Description of model	Numerical formulation	GUI support[a]	Provider[b]	Reference
ARMOS	Areal multiphase organic simulator program	Finite element	Yes	Environmental Systems Technologies, Inc.	Kaluarachchi *et al.* (1990)
MAGNAS	A multidimensional finite element transport of water, NAPL and air through porous media.	Finite element	Yes	HydroGeoLogic Inc.	Huyakorn *et al.* (1992)
MOFAT	A two-dimensional finite element program for multiphase flow and multicomponent transport	Finite element	Yes	USEPA	Katyal *et al.* (1991)
NAPL simulator	A subsurface flow and transport mathematical model for movement and fate of NAPL contaminants in near-surface granular soils	Finite element	No	USEPA	Guarnaccia *et al.* (1997)
STOMP	Subsurface transport over multiple phases model	Finite difference	Yes	Pacific Northwest National Laboratory	Oostrom *et al.* (2007)
TOUGH2v2	A numerical simulator for nonisothermal flows of multicomponent, multiphase fluids in one, two and three-dimensional porous and fractured media	Finite difference	Yes	Lawrence Berkeley National Laboratory	Pruess *et al.* (1999)
UTCHEM	A three-dimensional chemical flood simulator	Finite difference	Yes	Center for Petroleum and Geosystems Engineering (University of Texas, Austin); USEPA	Center for Petroleum and Geosystems Engineering (2000)
VENT2D	A multi-compound vapor transport and phase distribution model	Finite difference	No	Benson	Benson (1994)

[a]GUI: Graphical User Interface. [b]USEPA: US Environmental Protection Agency

particular method can easily support the strengths of their preferred solution strategy (Simpson and Clement, 2003). On top of that, we believed that modelers are always looking for the most up-to-date and user-friendly codes concerning the type of NAPL under investigation.

Karapanagioti *et al.* (2003) have found that only two codes (i.e., MOFAT and NAPL Simulator) include degradation as an important attenuation mechanism. NAPL Simulator has been used before (Kamon *et al.*, 2006) to predict the behavior of benzene under fluctuating groundwater table conditions. Unlike NAPL Simulator, MOFAT is capable of handling the presence of multicomponent mixtures in the subsurface.

The MOFAT numerical code is a two-dimensional model for coupled multiphase flow and multicomponent transport in planar or radially symmetric vertical sections (Katyal *et al.*, 1991). This program was developed based on mathematical models of multiphase flow (Kaluarachchi and Parker, 1989) and extensions of multicomponent constituent transport (Kaluarachchi *et al.*, 1992). The flow and transport of the three fluid phases (water, NAPL and gas) are considered in separate flow and transport modules by the program. Up to five components can partition between these three phases with equilibrium or kinetically controlled mass transfer. Advection, dispersion and diffusion of all phases are taken into account in two dimensions. Sorption and degradation are possible in all phases. Relationships between phase permeability, saturation and pressure are described by a three-phase extension of the Van Genuchten model. Previous studies using MOFAT

have been reported by a number of researchers (Gaganis *et al.*, 2002, 2004; Helweg and Ballantyne, 1992; Lenhard *et al.*, 1995; Steffy *et al.*, 1998; Tyagi and Martell, 1993). Development of MOFAT was based on previous numerical modeling (Kaluarachchi and Parker, 1989; Kuppusamy *et al.*, 1987; Parker, 1989; Parker *et al.*, 1987), experimental validation exercises (Lenhard *et al.*, 1988, 1991; Lenhard and Parker, 1988) and extended numerical models (Kaluarachchi and Parker, 1990, 1992).

Currently, the MOFAT numerical code is available with Windows Graphical User Interface (GUI). The program consists of the MOFAT numerical model, the MOFAT Pre-processor, Mesh Editor and the MOFAT Post-processor. Each relies on the other for data input and output. The typical input parameters are shown in Table 7 and more details control parameters are available in the MOFAT for Windows manual.

Simulation of LNAPL: Several numerical models have been used in model validation and verification involving quantitative experiments. The selection of numerical models for NAPL simulation is highly dependent on the multiphase flow model and transport model offered by the code. The free public domain codes are mostly the older versions that do not have user-friendly interfaces; for several of the latest versions, codes with graphical user interfaces (GUIs) are obtained at some cost. MDH Engineered Solutions Corporation (2005) has provided a report of model evaluations including those for NAPL simulation. The report involved rating modeling codes

Table 7: Typical input parameters and the abbreviation for MOFAT with Windows GUI[a]

Parameter	Abbreviation
Component/species properties:	
Oil-water partition coefficient (Γ_{wo})	GAM1
Air-water partition coefficient ($\Gamma_{\alpha a}$)	GAM2
Initial water phase concentration for species (K)	CINIT
Water-phase diffusion coefficient ($D^{\circ}_{\alpha w}$)	DIFW
Oil-phase diffusion coefficient ($D^{\circ}_{\alpha 0}$)	DIFO
Air-phase diffusion coefficient ($D^{\circ}_{\alpha a}$)	DIFA
Liquid density of pure species (ρ_{α})	DLIQ
Bulk fluid properties:	
Viscosity ratio (η_{ro})	VISOW
Oil-phase specific gravity (ρ_{ro})	RHOW
Air-oil scaling coefficient (β_{ao})	BAO
Oil-water scaling coefficient (β_{ow})	BOW
Transport properties:	
Longitudinal dispersivity (A_L)	TRANS1
Transverse dispersivity (A_T)	TRANS2
Soil properties:	
Horizontal saturated conductivity (K_{swx})	KSWX
Vertical saturated conductivity (K_{swz})	KSWZ
Soil porosity (ϕ)	POROS
Residual water saturation (S_m)	RESIW
Residual oil saturation (S_{or})	RESIO
Van Genutchen parameter (α)	ALPHA
Van Genutchen parameter (n)	PARAN

[a]GUI: Graphical user interface

based on 17 objective criteria. All the highly ranked codes were suitable for modeling the fate and transport of hydrocarbons if vapor phase transport was excluded as a requirement. During the ranking procedure, limited emphasis was placed on the ability to account for vapor/solid/liquid partitioning. Typically, codes that are designed to predict vapor phase partitioning are not designed to simulate the movement of dissolved hydrocarbons in both the unsaturated and the saturated zones. MDH initially recommended that a separate code be used to determine the amount of hydrocarbon that partitions into the aqueous and vapor phases.

In addition to this report, a review from Karapanagioti *et al.* (2003) for codes and usage in modeling attenuation of volatile organic compounds (VOCs) was also helpful in selecting suitable numerical models. In general, the majority of the codes in their discussion describe the transport and fate of contaminants dissolved in the aqueous phase. Models that account for transport in the saturated zone usually include a limited number of processes (i.e., advection and dispersion). Only a few of these models include air-water partitioning and transport (i.e., diffusion and/or advection) in the gas phase and are thus capable of modeling VOCs. As their reviews are limited to VOC modeling, Non-Volatile Three-Phase (NVTP) operational codes such as STOMP are not considered.

Another difficulty encountered with the unsaturated zone relates to uncertainty of chemical properties, usually unknown temperature dependence (Karapanagioti *et al.*, 2003). Most properties (for examples, Table 3 and 4) are assumed at room temperature (i.e., 20°C) and their relevance to soil contamination or thermodynamic relations has probably not been experimentally investigated.

Host-Madsen and Jensen (1992) used ECLIPSE to model saturation of wetting fluid (S-P of water-air, NAPL-air and water-NAPL). They produced contour lines of measured and simulated NAPL saturation, water and NAPL saturation and NAPL travel-time after a spill. The measured and simulated NAPL saturation comparisons were agreed reasonably well.

Van Geel and Sykes (1997) used IMPES and found similarities between measured and modeled pressures, as well as relatively small differences between calculated and modeled water saturations. Waddil and Parker (1997) used ARMOS and showed agreement between measured and predicted cumulative oil recovery. The observed and predicted vertical oil saturation came into reasonable agreement at early times during the recovery process and showed greater departure at the later time.

In the absence of analytical solutions for transient three-phase fluid movement, Lenhard *et al.* (1995) used a published code of MOFAT. A good agreement was found between STOMP results and MOFAT-2D for NAPL and water phase saturations and also between simulation and experimental results of NAPL and water phase saturation. By using STOMP, Schroth *et al.* (1998b) have shown reasonable agreement between experimental and simulated NAPL saturation distributions. However, discrepancies between predicted VGM and BCB models were attributed to differences in the S-P and k-S relations. Using the same code, Wipfler *et al.* (2004) performed sensitivity analysis by varying LNAPL infiltration rate, the capillarity contrast at the fine to coarse interface (i.e., Van Genuchten parameter) and the inclination of the layered sand. The results indicated that the qualitative LNAPL redistribution is mainly subjected to the capillarity contrast between sands. A greater contrast gave more horizontal migration of LNAPL. The infiltration into the coarse sand layer always occurs at the same level compared to the water table, for various inclinations and various initial fluxes. In Oostrom *et al.* (2006b), the STOMP simulator was used to simulate LNAPL saturations after 30 days, 45 days and 1 year by considering or not considering residual and

entrapped NAPL as well as water table rise. The predicted and observed residual saturation formation showed good agreement and has limited upward LNAPL movement after the water table rise.

Visualization of results: The purposes of analysis include cross-validation, validation and verification exercises and model prediction for assessment. The shape and extent of NAPL saturation plumes, travel-time and-distance of 2-D NAPL flow and fluid-phase concentrations as well as *S-P* relationships comprise the common interests of most NAPL researchers.

Visualization of results is the product of the numerical simulations that provide essential illustrations for model assessment. Regardless of dimensionality of model use, visualization requires sophisticated IT tools that can address tasks beyond simple pre- and post-processing of simulation (Wheeler and Peszynska, 2002). Some of the original codes for NAPL modeling do not provide the visualization results directly, with graphic results produced only by post-processing. Therefore, to visualize the contours result for NAPL saturation, external software such as Surfer® is frequently needed. Perhaps future integrated environmental web-based software could help model developers produce high quality images and animations. In addition, the new advancement in MATLAB® family products resulting from their latest release may provide better data visualization with some updated toolboxes to provide a high-end visualization.

SUMMARY AND FUTURE RESEARCH

The two-dimensional non-aqueous phase liquid experiments were discussed with the application of light reflection and light transmission methods associated with image analysis methods. The experiments followed by numerical simulations were emphasized to show that data acquisition is essential for verification and validation of numerical models.

Due to the toxic nature of the chemicals spilled at site modeling was used to study LNAPL transport in the subsurface. The interest in carrying out laboratory and numerical simulations on LNAPL in the unsaturated zone was shown by the encouraging reviews of previous 2-D multiphase flow numerical models for NAPL in unsaturated porous media. As NAPL contamination data were typically difficult and very expensive to acquire, we recommend improving laboratory techniques, especially NAPL saturation imaging techniques such as photographic methods. In addition, enhanced numerical simulations for better future model predictions and high-end visualization of results were sorely needed.

Acquisition of fluid saturation and pressure data was the most essential in numerical model validation and verification. Without the transient pressure and saturation data, there would be insufficient constitutive relations for model prediction. The two-phase air-water P-S relationship was used to produce the three-phase constitutive relationships between fluid permeability, saturation and pressure (k-S-P).

As more researchers come to prefer non-destructive and non-intrusive techniques, the LTM, the LRM and the MIAM were alternatives that acquire images by using either a digital camera or video camera and image processing techniques. The Image-Pro Plus software (Media Cybernetics Inc.) and MATLAB® with an up-to-date toolbox were the popular choices for image processing.

Depending on the type of LNAPL source, MOFAT and STOMP were found widely used codes for numerical simulations of the 2-D multiphase flow problems. The visualization of results for final assessment of every simulation can be done with either Surfer® or MATLAB®, however each

visualization technique required some improvement in future research. In conclusion, future laboratory and numerical simulations should consider the present technologies involved in this field.

ACKNOWLEDGMENTS

REFERENCES

Bear, J., 1972. Dynamics of Fluids in Porous Media. 1st Edn., American Elsvier, New York.

Benson, D.A., 1994. Users manual to VENT2D: A multi-compound vapor transport and phase distribution model. Claremont St.: Reno, Nevada. ftp://ftp.scs.unr.edu/pub/classes/daveb/vent2d/v2dman.pdf.

Benson, D.A., D. Huntley and P.C. Johnson, 1993. Modeling vapor extraction and general transport in the presence of NAPL mixtures and nonideal conditions. Ground Water, 31: 437-445.

Bob, M.M., M.C. Brooks, S.C. Mravik and A.L. Wood, 2008. A modified light transmission visualization method for DNAPL saturation measurements in 2-D models. Adv. Water Resour., 31: 727-742.

Bridge, J.W., S.A. Banwart and A.L. Heathwaite, 2006. Noninvasive quantitative measurement of colloid transport in mesoscale porous media using time lapse fluorescence imaging. Environ. Sci. Technol., 40: 5930-5936.

Broorks, R.H. and C.T. Corey, 1964. Hydraulic properties of porous media. Hydrology, Paper3.Colorado State University, Fort Collins, pp: 27.

Burdine, N.T., 1953. Relative permeability calculations from pore-size distribution data. Trans. AIME, 198: 71-78.

Catalan, L.J.J. and F.A.L. Dullien, 1995. Application of gravity drainage to the recovery of residual LNAPL in homogeneous and lensed sand packs. J. Contam. Hydrol., 18: 279-306.

Center for Petroleum and Geosystems Engineering, 2000. Technical documentation for UTCHEM-9.0, A three-dimensional chemical flood simulator. Volume II: The University of Texas at Austin: Texas. http://www.cpge.utexas.edu/utchem/UTCHEM_Tech_Doc.pdf.

Chevalier, L.R., 1998. Experimental and numerical evaluation of lnapl lens and polluted capillary fringe thickness. J. Environ. Eng., 124: 156-161.

Chevalier, L.R. and J. Petersen, 1999. Literature review of 2-D laboratory experiments in NAPL flow, transport and remediation. Soil Sediment Contam., 8: 149-167.

Chevron Philips Chemical Company LP, 2009. Material safety data sheet. Soltrol 220 Isoparaffin Solvent. http://www.cpchem.com/msds/100000067798_SDS_US_EN.PDF.

Conrad, S.H., R.J. Glass and W.J. Peplinski, 2002. Bench-scale visualization of DNAPL remediation processes in analog heterogeneous aquifers: Surfactant floods and *in situ* oxidation using permanganate. J. Contam. Hydrol., 58: 13-49.

Corey, A.T., 1994. Mechanics of Immiscible Fluids in Porous Media. Water Resources Publication, Algeria.

Darnault, C.J.G., J.A. Throop, D.A. Dicarlo, A. Rimmer, T.S. Steenhuis and J.Y. Parlange, 1998. Visualization by light transmission of oil and water contents in transient two-phase flow fields. J. Contam. Hydrol., 31: 337-348.

Darnault, C.J.G., D.A. DiCarlo, T.W.J. Bauters, A.R. Jacobson and J.A. Throop *et al.*, 2001. Measurement of fluid contents by light transmission in transient three-phase oil-water-air systems in sand. Water Resour. Res., 37: 1859-1868.

Fetter, C.W., 1999. Contaminant Hydrogeology. Prentice Hall, New Jersey.

Flores, G., T. Katsumi and M. Kamon, 2007. Evaluation of LNAPL migration under fluctuating groundwater by image analysis. Ann. Disaster Prevention Res. Inst., 50: 399-405.

Gaganis, P., H.K. Karapanagioti and V.N. Burganos, 2002. Modeling multicomponent NAPL transport in the unsaturated zone with the constituent averaging technique. Adv. Water Resour., 25: 723-732.

Gaganis, P., P. Kjeldsen and V.N. Burganos, 2004. Modeling natural attenuation of multicomponent fuel mixtures in the vadose zone: Use of field data and evaluation of biodegradation effects. Vadose Zone J., 3: 1262-1275.

Gelhar, L.W., C. Welty and K.R. Rehfeldt, 1992. A critical review of data on field scale dispersion in aquifers. Water Resour. Res., 28: 1955-1974.

Glass, R.J., S.H. Conrad and W. Peplinski, 2000. Gravity-destabilized nonwetting phase invasion in macroheterogeneous porous media: Experimental observations of invasion dynamics and scale analysis. Water Resour. Res., 36: 3121-3137.

Guarnaccia, J., G. Pinder and M. Fishman, 1997. NAPL: Simulator documentation. NRMRL USEPA: Ada, Oklahoma.

Helweg, O.J. and D.B. Ballantyne, 1992. Migration of spilled oil from ruptured underground crude oil pipelines in the Memphis area. Lifeline Earthquake Engineering in the Central and Eastern US, 09/92; pp. 140-152. http://md1.csa.com/partners/viewrecord.php?requester=gs&collection =TRD&recid=0010187EN.

Hoa, N.T., 1981. A new method allowing the measurement of rapid variations of the water content in sandy porous media. Water Resour. Res., 17: 41-48.

Hochmuth, D.P. and D.K. Sunada, 1985. Ground-water model of two-phase immiscible flow in coarse material. Ground Water, 23: 617-626.

Host-Madsen, J. and K.H. Jensen, 1992. Laboratory and numerical investigations of immiscible multiphase flow in soil. J. Hydrol., 135: 13-52.

Huyakorn, P.S., Y.S. Wu, S. Panday and N.S. Park, 1992. MAGNAS3: Multiphase Analysis of Groundwater, Non-Aqueous Phase Liquid and Soluble Component. Version 1.0., HydroGeoLogic Inc., Herndon, VA.

Illangasekare, T.H., E.J. Armbruster and D.N. Yates, 1995. Non-aqueous-phase fluids in heterogeneous aquifers-Experimental study. J. Environ. Eng., 121: 571-579.

Kaluarachchi, J.J. and J.C. Parker, 1989. An efficient finite element method for modeling multiphase flow. Water Resour. Res., 25: 43-54.

Kaluarachchi, J.J. and J.C. Parker, 1990. Modeling multicomponent organic chemical transport in three-fluid-phase porous media. J. Contam. Hydrol., 5: 349-374.

Kaluarachchi, J.J., J.C. Parker and R.J. Lenhard, 1990. A numerical model for areal migration of water and light hydrocarbon in unconfined aquifers. Adv. Water Resour., 13: 29-40.

Kaluarachchi, J.J. and J.C. Parker, 1992. Multiphase flow with a simplified model for oil entrapment. Trans. Porous Media, 7: 1-14.

Kaluarachchi, J.J., J.C., Parker and R.J. Lenhard, 1992. Modeling flow in three fluid phase porous media with nonwetting fluid entrapment. Proceedings of the International Conference on Subsurface Contamination by Immiscible Fluids, (SCIF'92), Calgary, pp: 141-147.

Kamon, M., Y. Li, G. Flores, T. Inui and T. Katsumi, 2006. Experimental and numerical study on migration of LNAPL under the influence of fluctuating water table in subsurface. Ann. Disaster Prevention Res. Inst., 49: 383-392.

Karapanagioti, H.K., P. Gaganis and V.N. Burganos, 2003. Modeling attenuation of volatile organic mixtures in the unsaturated zone: Codes and usage. Environ. Modell. Software, 18: 329-337.

Katyal, A.K., J.J. Kaluarachchi, J.C. Parker, J.S. Cho and L.G. Swaby, 1991. MOFAT: A two dimensional finite element program for multiphase flow and multicomponent transport. Program Documentation, Version, RSKERL USEPA: Ada, Oklahoma.

Kechavarzi, C., K. Soga and P. Wiart, 2000. Multispectral image analysis method to determine dynamic fluid saturation distribution in two-dimensional three-fluid phase flow laboratory experiments. J. Contam. Hydrol., 46: 265-293.

Kechavarzi, C., K. Soga and T.H. Illangasekare, 2005. Two-dimensional laboratory simulation of LNAPL infiltration and redistribution in the vadose zone. J. Contam. Hydrol., 76: 211-233.

Kechavarzi, C., K. Soga, T.H. Illangasekare and P. Nikolopoulos, 2008. Laboratory study of immiscible contaminant flow in unsaturated layered sands. Vadose Zone J., 7: 1-9.

Konz, M., P. Ackerer, E. Meier, P. Huggenberger, E. Zechner and D. Gechter, 2008. On the measurement of solute concentrations in 2-D flow tank experiments. Hydrol. Earth Syst. Sci., 12: 727-738.

Kuppusamy, T., J. Sheng, J.C. Parker and R.J. Lenhard, 1987. Finite-element analysis of multiphase immiscible flow through soils. Water Resour. Res., 23: 625-631.

Lahvis, M.A. and A.L. Baehr, 1997. Documentation of R-UNSAT, a computer model for the simulation of reactive, multispecies transport in the unsaturated zone. U. S. Geological Survey Open-File Report 97-630, pp: 104.

Lenhard, R.J. and J.C. Parker, 1988. Experimental validation of the theory of extending two-phase saturation-pressure relations to three-fluid phase systems for monotonic drainage paths. Water Resour. Res., 24: 373-380.

Lenhard, R.J., J.H. Dane, J.C. Parker and J.J. Kaluarachchi, 1988. Measurement and simulation of one-dimensional transient three-phase flow for monotonic liquid drainage. Water Resour. Res., 24: 853-863.

Lenhard, R.J., J.C. Parker and J.J. Kaluarachchi, 1991. Comparing simulated and experimental hysteretic two-phase transient fluid flow phenomena. Water Resour. Res., 27: 2113-2124.

Lenhard, R.J., M. Oostrom and M.D. White, 1995. Modeling fluid flow and transport in variably saturated porous media with the STOMP simulator. 2. Verification and validation exercises. Adv. Water Resour., 18: 365-373.

Leverett, M.C., 1941. Capillary behavior in porous Media. Trans. AIME, 142: 341-358.

Lewis, R.W. and B.A. Schrefler, 1998. The Finite Element Method in the Static and Dynamic Deformation and Consolidation of Porous Media. John Wiley and Sons, London, UK.

Lewis, R.W., B.A. Schrefler and N.A. Rahman, 1998. A finite element analysis of multiphase immiscible flow in deforming porous media for subsurface systems. Commun. Numer. Methods Eng., 14: 135-149.

MDH Engineered Solutions Corporation, 2005. Evaluation of computer models for predicting the fate and transport of hydrocarbons in soil and groundwater. The Water Research Users Group, Alberta Environment. http://environment.gov.ab.ca/info/library/6682.pdf.

McCarthy, K.A., 1992. The transport of volatile compounds across the capillary fringe. Ph.D. Thesis, Oregon Graduate Institute of Science and Technology, Oregon.

McCarthy, K.A. and R.L. Johnson, 1993. Transport of volatile organic compounds across the capillary fringe. Water Resour. Res., 29: 1675-1683.

McDowell, C.J. and S.E. Powers, 2003. Mechanisms affecting the infiltration and distribution of ethanol-blended gasoline in the vadose zone. Environ. Sci. Technol., 37: 1803-1810.

McNeil, J.D., G.A. Oldenborger and R.A. Schincariol, 2006. Quantitative imaging of contaminant distributions in heterogeneous porous media laboratory experiments. J. Contam. Hydrol., 84: 36-54.

Mercer, J.W. and R.M. Cohen, 1990. A review of immiscible fluids in the subsurface: Properties, models, characterization and remediation. J. Contam. Hydrol., 6: 107-163.

Mualem, Y., 1976. A new model for predicting the hydraulic conductivity of unsaturated porous media. Water Resour. Res., 12: 513-522.

Niemet, M.R. and J.S. Selker, 2001. A new method for quantification of liquid saturation in 2D translucent porous media systems using light transmission. Adv. Water Resour., 24: 651-666.

O'Carroll, D.M., S.A. Bradford and L.M. Abriola, 2004. Infiltration of PCE in a system containing spatial wettability variations. J. Contam. Hydrol., 73: 39-63.

Oostrom, M., C. Hofstee and J.H. Dane, 1997. Light nonaqueous-phase liquid movement in a variably saturated sand. Soil Sci. Soc. Am. J., 61: 1547-1554.

Oostrom, M., C. Hofstee and T.W. Wietsma, 2006a. Behavior of a viscous LNAPL under variable water table conditions. Soil Sediment Contam. Int. J., 15: 543-564.

Oostrom, M., J.H. Dane and T.W. Wietsma, 2006b. A review of multidimensional, multifluid intermediate-scale experiments: Nonaqueous phase liquid dissolution and enhanced remediation. Vadose Zone J., 5: 570-598.

Oostrom, M., J.H. Dane and T.W. Wietsma, 2007. A review of multidimensional, multifluid, intermediate-scale experiments: Flow behavior, saturation imaging and tracer detection and quantification. Vadose Zone J., 6: 610-637.

Pantazidou, M. and N. Sitar, 1993. Emplacement of nonaqueous liquids in the vadose zone. Water Resour. Res., 29: 705-722.

Parker, J.C., R.J. Lenhard and T. Kuppusamy, 1987. A parametric model for constitutive properties governing multiphase flow in porous media. Water Resour. Res., 23: 618-624.

Parker, J.C., 1989. Multiphase flow and transport in porous media. Rev. Geophys., 27: 311-328.

Pruess, K., G.J. Moridis and C. Oldenburg, 1999. TOUGH2 Users Guide, Version 2.0. Lawrence Berkeley National Laboratory, California.

Rahman, N.A. and R.W. Lewis, 1999. Finite element modelling of multiphase immiscible flow in deforming porous media for subsurface systems. Comput. Geotech., 24: 41-63.

Rahman, N.A., S.A. Kamaruddin and B.A. Schrefler, 2001. Numerical modelling of thermo-hydro mechanical (THM) in deforming porous media for subsurface systems. J. Teknologi, 34: 31-44.

Rahman, N.A., S.A. Kamaruddin and B.A. Schrefler, 2002. Computer modelling of thermo-hydro mechanical (THM) in subsurface systems. IEM J., 63: 48-55.

Ravi, V. and J.A. Johnson, 1997. VLEACH-A one-dimensional finite difference vadose zone leaching model, Version 2.2. Center for Subsurface Modeling Support, USEPA RSKERL, Ada, OK.

Sakari, M., M.P. Zakaria, M.B.M. Junos, N.A. Annuar and H.Y. Yun *et al.*, 2008. Spatial distribution of petroleum hydrocarbon in sediments of major rivers from east coast of Peninsular Malaysia. J. Coastal Marine Sci., 32: 9-18.

Saleem, M., M.S. Al-Suwaiyan, S.A. Aiban, A.M. Ishaq, M.H. Al-Malack and M. Hussain, 2004. Estimation of spilled hydrocarbon volume-The state-of-the-art. Environ. Technol., 25: 1077-1090.

Schincariol, R.A. and F.W. Schwartz, 1990. An experimental investigation of variable density flow and mixing in homogeneous and heterogeneous media. Water Resour. Res., 26: 2317-2329.

Schincariol, R.A., E.E. Herderick and F.W. Schwartz, 1993. On the application of image analysis to determine concentration distributions in laboratory experiments. J. Contam. Hydrol., 12: 197-215.

Schroth, M.H., S.J. Ahearn, J.S. Selker and J.D. Istok, 1996. Characterization of miller-similar silica sands for laboratory hydrologic studies. Soil Sci. Soc. Am. J., 60: 1331-1339.

Schroth, M.H., J.D. Istok and J.S. Selker, 1998a. Three-phase immiscible fluid movement in the vicinity of textural interfaces. J. Contam. Hydrol., 32: 1-23.

Schroth, M.H., J.D. Istok, J.S. Selker, M. Oostrom and M.D. White, 1998b. Multifluid flow in bedded porous media: Laboratory experiments and numerical simulations. Adv. Water Resour., 22: 169-183.

Schwille, F., 1967. Petroleum contamination of the subsoil: A hydrological problem. Proceedings of Symposium on the Joint Problems of the Oil and Water Industries: Hotel Metropole, Jan. 18–20, London, pp: 23-54.

Simmons, C.S., J.F. McBride, J.W. Cary and R.J. Lenhard, 1992. Organic liquid infiltration into unsaturated porous media. Proceedings of the International Conference on Subsurface Contamination by Immiscible Fluids, April 18-20, Calgary, pp: 213-219.

Simpson, M.J. and T.P. Clement, 2003. Comparison of finite difference and finite element solutions to the variably saturated flow equation. J. Hydrol., 270: 49-64.

Steffy, D.A., C.D. Johnston and D.A. Barry, 1998. Numerical simulations and long-columntests of LNAPL displacement and trapping by a fluctuating water table. Soil Sediment Contam. Int. J., 7: 325-356.

Tidwell, V.C. and R.J. Glass, 1994. X ray and visible light transmission for laboratory measurement of two-dimensional saturation fields in thin-slab systems. Water Resour. Res., 30: 2873-2882.

Tindall, J.A. and J.R. Kunkel, 1999. Unsaturated Zone Hydrology for Scientists and Engineers. Prentice Hall, New Jersey.

Tyagi, A.K. and J. Martell, 1993. Fate/transport modeling of immiscible LNAPL in unsaturated aquifers. Proceedings of the Symposium on Engineering Hydrology, (SEH'93), New York, pp: 701-705.

USEPA, 1991. Subsurface Contamination Reference Guide. USEPA, Washington, DC., pp: 13.

Van Geel, P.J. and J.F. Sykes, 1994a. Laboratory and model simulations of a LNAPL spill in a variably-saturated sand. 1. Laboratory experiment and image analysis techniques. J. Contam. Hydrol., 17: 1-25.

Van Geel, P.J. and J.F. Sykes, 1994b. Laboratory and model simulations of a LNAPL spill in a variably-saturated sand. 2. Comparison of laboratory and model results. J. Contam. Hydrol., 17: 27-53.

Van Geel, P.J. and J.F. Sykes, 1997. The importance of fluid entrapment, saturation hysteresis and residual saturations on the distribution of a lighter-than-water non-aqueous phase liquid in a variably saturated sand medium. J. Contam. Hydrol., 25: 249-270.

Van Genuchten, M.T., 1980. A closed-form equation for predicting the hydraulic conductivity of unsaturated soils. Soil Sci. Soc. Am. J., 44: 892-898.

Waddill, D.W. and J.C. Parker, 1997. Recovery of light, non-aqueous phase liquid from porous media: Laboratory experiments and model validation. J. Contam. Hydrol., 27: 127-155.

Weisbrod, N., M.R. Niemet and J.S. Selker, 2003. Light transmission technique for the evaluation of colloidal transport and dynamics in porous media. Environ. Sci. Technol., 37: 3694-3700.

Wheeler, M.F. and M. Peszynska, 2002. Computational engineering and science methodologies for modeling and simulation of subsurface applications. Adv. Water Resour., 25: 1147-1173.

White, M.D., M. Oostrom and R.J. Lenhard, 1995. Modeling fluid flow and transport in variably saturated porous media with the STOMP simulator. 1. Nonvolatile three-phase model description. Adv. Water Resour., 18: 353-364.

White, M.D. and M. Oostrom, 1997. STOMP, subsurface transport over multiple phases: Users guide. Pacific Northwest National Laboratory Report PNNL-11218. Pacific Northwest National Laboratory: Washington, DC. http://www.osti.gov/bridge/product.biblio.jsp?osti_id=553734.

White, M.D. and M.S. Oostrom, 2000. Subsurface transport over multiple phases: Version 2.0. PNNL Report 12034, Pacific Northwest National Laboratory, Richland, Washington.

Wipfler, E.L., M. Ness, G.D. Breedveld, A. Marsman and S.E. van der Zee, 2004. Infiltration and redistribution of LNAPL into unsaturated layered porous media. J. Contam. Hydrol., 71: 47-66.

Zakaria, M.P., H. Takada, S. Tsutsumi, K. Ohno, J. Yamada, E. Kouno and H. Kumata, 2002. Distribution of polycyclic aromatic hydrocarbons (PAHs) in rivers and estuaries in Malaysia: Widespread imput of petrogenic PAHs. Environ. Sci. Technol., 36: 1907-1918.